# A VISCOUS MODEL FOR LUBRICANT TRANSFER FROM MEDIA TO HEAD DURING HEAT-ASSISTED MAGNETIC RECORDING (HAMR)

By

Siddhesh Vivek Sakhalkar

B.Tech. (Indian Institute of Technology, Bombay) 2014

A report submitted in partial satisfaction of the
requirements for the degree of
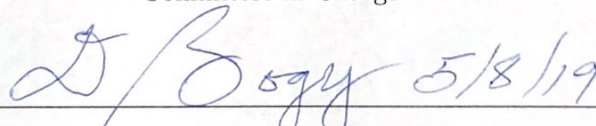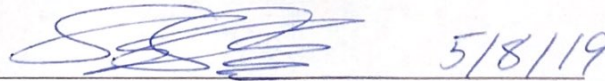
Masters of Science, Plan II

in

Mechanical Engineering

at the

University of California at Berkeley

Committee in Charge:

_____
Professor David B. Bogy, Chair

_____
Professor Shawn C. Shadden

Spring 2019

**Abstract**

A Viscous Model for Lubricant Transfer from Media to Head during Heat-Assisted

Magnetic Recording (HAMR)

by

Siddhesh V. Sakhalkar

Master of Science in Engineering – Mechanical Engineering

University of California, Berkeley

Professor David B. Bogy, Chair

Heat-Assisted Magnetic Recording (HAMR) is widely viewed as a technology that is essential to achieve storage densities beyond 1 Tb/in$^2$ in hard disk drives[1]. While traditional magnetic media is thermally unstable at room temperature for the small bit sizes needed for high density recording, the high coercivity HAMR magnetic media can safely store data at very small bit sizes of $\sim (25 \text{ nm})^2$. In order to write on the high coercivity media, a complex laser delivery system integrated into the magnetic head is used to locally heat the HAMR recording bit to its Curie temperature ($\sim 500$ ºC) within a few nanoseconds, thereby reducing its coercivity. However, reliability of the head-disk interface (HDI) during high temperature transient laser heating still remains a major challenge that needs to be addressed before HAMR can be made into a robust commercial product[2].

One of the challenges in HAMR is the creation of write-induced contamination at the near field transducer (NFT) on the head. While the peak disk temperature during HAMR writing is $\sim 500$ ºC, the peak temperature of the head is much lower ($\sim 310$ ºC)[3]. This temperature difference causes the polymer lubricant, which covers and protects the disk, to evaporate, form vapor in the HDI and subsequently condense on the relatively cooler head. The lubricant acts as a carrier, causing a continuous deposition of media contaminants at the head NFT. In this study, we develop a viscous continuum model that predicts the disk-to-head lubricant transfer during HAMR writing. The model simultaneously determines the thermo-capillary shear stress driven deformation and evaporation of the lubricant film on the disk, the convection and diffusion of the vapor phase lubricant in the air bearing and the evolution of the condensed lubricant film on the slider. The model also considers molecular interactions between disk-lubricant, slider-lubricant and lubricant-lubricant in terms of disjoining pressure.

**Acknowledgments**

I would like to express my sincere gratitude to my advisor, Prof. David B. Bogy for his continuous guidance and support throughout this work. Thanks to Prof. Shawn Shadden for reviewing this work. I would like to thank my partner, Anushka Gupta and my family for their immense support. I would also like to thank my friends at the Computer Mechanics Laboratory (CML) for their help and support.

# Contents

# List of Figures

# Chapter 1

# Introduction

The demand for data storage is increasing rapidly with the increase in the number and size of the information that we are generating and keeping. Much of the world's digital information has been and still is stored on hard disk drives (HDDs). While HDDs may appear to be giving way to solid state drives (SSDs) in many smart phones and laptops, much of our digital data is actually stored on cloud storage services, which are enormous arrays of HDDs connected on a network, maintained by the cloud service provider. Simplistically, a HDD consists of a magnetic disk (also known as media) which stores data and a magnetic head (also known as slider) which flies over the rotating disk and reads/writes data onto it. In between the head and the disk, there is a column of air, known as the air bearing. To prevent wear & tear of the disk/head, it is customary to apply a coating of a polymer lubricant on the disk. The minimum head-disk clearance in HDDs has reduced from a few microns ($\sim$ 40 years ago) to $<$ 10 nm today. This necessitates the lubricant film in contemporary HDDs to have a thickness of only 1-2 nm.

Current HDD products have approached upto 1 Tb/in$^2$ storage density. Higher storage densities will soon no longer be possible with convectional recording technologies due to the superparamagnetic limit: if the size of the magnetic media bits is further decreased, the bits will become thermally unstable. Heat-Assisted Magnetic Recording (HAMR) offers to overcome this obstacle by using magnetic media material with a high coercivity (coercivity is the ability of a material to maintain its magnetic domains and withstand any undesired external magnetic influences). This enables the HAMR media to safely store data at very small bit sizes of $\sim$ (25 nm)$^2$. The coercivity of a material is temperature dependent. If the temperature of a magnetized material is increased above its Curie temperature, its coercivity will become much lower, until it has cooled down. HAMR utilizes this property

to write on the high coercivity media by using a complex laser delivery system integrated into the magnetic head to locally heat the HAMR recording bit to its Curie temperature ($\sim$ 500 °C) within a few nanoseconds. However, reliability of the head-disk interface (HDI) during high temperature transient laser heating still remains a major challenge that needs to be addressed before HAMR can be made into a robust commercial product[2]. One of the tribological challenges in HAMR is the formation of write-induced head contamination at the near field transducer (NFT - a component inside the HAMR head used to focus the laser beam onto the disk)[3]. Kiely et al.[3] reported that this contamination begins soon after the laser power is turned on ($<$ 1 second) and grows over time until the contamination height reaches the head-disk clearance. Once the head contamination contacts the media surface, the disk motion generates a smear down-track of the NFT.

One possible mechanism that has been proposed for HAMR contamination is lubricant transfer from the disk to the head through thermodynamic driving forces[3]. While the peak media temperature during HAMR writing is $\sim$ 500 °C, the peak temperature of the head is $\sim$ 310 °C[3]. This temperature difference causes the lubricant to evaporate from the disk, form vapor in the HDI and condense on the relatively cooler head. The lubricant acts as a carrier, causing a continuous deposition of contaminants originating from the media at the head NFT. Xiong et al.[4] also reported similar deposition of materials on the head after HAMR writing. They observed that after the NFT was turned off and the head-media temperature difference was inverted, material was transfered from the head back to the media. This indicates that the temperature difference between the head and the media is an important mechanism for the material transfer.

Understanding the mechanism of disk-to-head lubricant and contaminant transfer is crucial in order to eliminate or control its effect and to develop reliable HAMR drives. During HAMR writing, there is a continuous circulation of lubricant between the disk, the air bearing and the slider. The depletion and deformation of disk lubricant, diffusion and convection of the vapor phase lubricant in the air bearing and the evolution of the deposited slider lubricant are strongly coupled and must be modeled simultaneously to understand the physics of the transfer process. In this study, we develop a viscous model that predicts the evolution of the disk lubricant film, the lubricant vapor phase in the air bearing and the slider lubricant film during HAMR writing. Our model considers the effects of thermocapillary stress, disjoining pressure, thin-film viscosity and evaporation/condensation on the behavior of lubricant in the HDI.

# Chapter 2

# Lubrication Theory

During HAMR writing, the media is locally heated to its Curie Temperature ($T_{max,d} \sim$ 500 °C). The high spatial temperature gradient ($\nabla T_d$) causes the lubricant film on the disk (thickness $h_d$) to deform and evaporate. Lubricant evaporation causes the partial pressure of the lubricant vapor in the air bearing, $p_v$ to rise. Some of this lubricant vapor condenses on the relatively cooler slider surface (maximum head temperature $T_{max,s} \sim 310$ °C)[3], depositing a thin lubricant film of thickness $h_s$. The spatial temperature gradient on the slider ($\nabla T_s$) causes this deposited lubricant film to deform. A schematic of this disk to slider lubricant transfer process is shown in Figure 2.1. The temperature profile of the disk $T_d(x, y, t)$ and the slider $T_s(x, y, t)$ is assumed to be known (a Gaussian profile with a peak of $T_{max,d}/T_{max,s}$ and FWHM of 20 nm). Thus, we have three unknown profiles in this problem - $h_d(x, y, t)$, $h_s(x, y, t)$ and $p_v(x, y, t)$. In this chapter, we drive the governing equations for these three unknown profiles using lubrication theory.

## 2.1   Governing Equation for Disk/Slider Lubricant

We consider the generic problem of a thin Newtonian lubricant film (with viscosity $\mu$) resting on a flat substrate moving at a constant speed $U$. The co-ordinate axes are defined such that the $z$ axis is along the lubricant thickness and the $x$ axis is along the direction of the substrate velocity $U$. The top surface of the lubricant is free to evolve under the influence of external shear stress $\boldsymbol{\tau} = \tau_x \boldsymbol{e_x} + \tau_y \boldsymbol{e_y}$ and external pressure $p$ and thus the lubricant thickness $h(x, y, t)$ is unknown. The fundamental assumption of lubrication theory is that the characteristic dimension in the thickness direction $h_0$ is much smaller than the characteristic dimension in the length and width directions, $L$ (i.e. $h_0 \ll L$). Additionally,
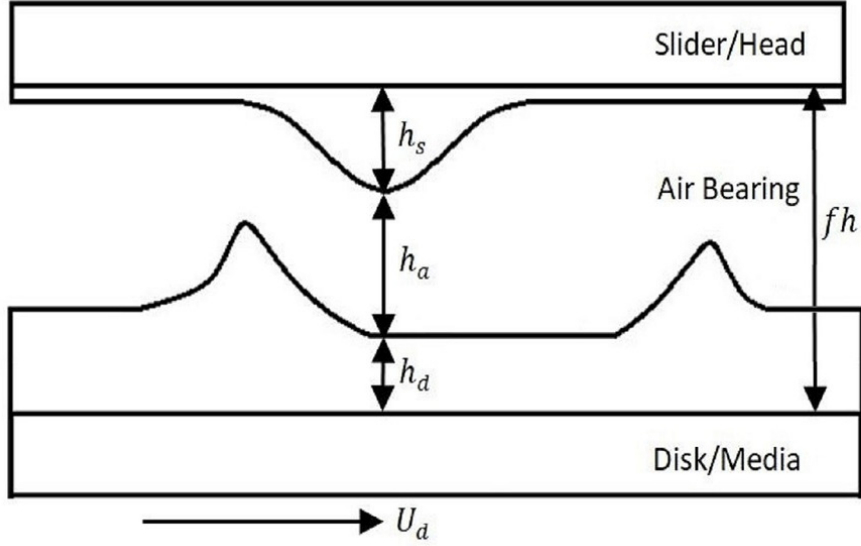
Figure 2.1: HAMR Lubricant Transfer Schematic: Lubricant film of thickness $h_d(x, y, t)$ on the disk is subjected to laser heating. The disk lubricant evaporates to form vapor having partial pressure $p_v(x, y, t)$ and density $\rho_v(x, y, t)$ in the HDI. The vapor condenses on the slider to form a film of thickness $h_s(x, y, t)$. Reprinted by permission from Springer Nature (Tribology Letters)[5], Copyright (2017).

the inertial terms in the equation of motion are assumed to be small compared to the viscous terms (i.e. low Reynols number flow) and the effect of gravity is assumed to be small. With these approximations, the Navier Stokes equations for the x and y velocity components $v_x$ and $v_y$ simplify to

$$
\frac{\partial p}{\partial x} = \frac{\partial}{\partial z}\left(\mu \frac{\partial v_x}{\partial z}\right)
$$
$$
\frac{\partial p}{\partial y} = \frac{\partial}{\partial z}\left(\mu \frac{\partial v_y}{\partial z}\right) \tag{2.1}
$$
$$
\frac{\partial p}{\partial z} = 0
$$

Here $\mu$ is the lubricant viscosity, $p$ is the lubricant pressure. Since $\frac{\partial p}{\partial z} = 0$, the pressure $p$ is independent of the normal co-ordinate $z$, i.e, $p \equiv p(x, y, t)$. We additionally assume that the lubricant viscosity also does not vary the the normal direction, i.e., $\mu \equiv \mu(x, y, t)$. Integrating Eq. (2.1) with this assumption and boundary conditions $v_x = U, v_y = 0$ at $z = 0$

and $\mu \frac{\partial v_x}{\partial z} = \tau_x$, $\mu \frac{\partial v_y}{\partial z} = \tau_y$ at $z = h$, we get:

$$v_x = \frac{1}{\mu} \frac{\partial p}{\partial x} \left( \frac{1}{2} z^2 - hz \right) + \frac{\tau_x}{\mu} z + U$$

$$v_y = \frac{1}{\mu} \frac{\partial p}{\partial y} \left( \frac{1}{2} z^2 - hz \right) + \frac{\tau_y}{\mu} z \tag{2.2}$$

Integrating the continuity equation for incompressible fluids $\nabla \cdot \boldsymbol{v} = 0$ across the film thickness $h$, we get

$$\frac{\partial h}{\partial t} + \frac{\partial q_x}{\partial x} + \frac{\partial q_y}{\partial y} + \frac{\dot{m}}{\rho_l} = 0$$

$$q_x = \int_0^h v_x dz \tag{2.3}$$

$$q_y = \int_0^h v_y dz$$

Here $\rho_l$ is the constant lubricant density and $\dot{m}$ is the mass flux due to evaporation. Inserting the velocity profiles from Eq. (2.2) into the integrated continuity equation (Eq. 2.3), we arrive at the governing evolution equation for the lubricant[6,7]

$$\frac{\partial h}{\partial t} + U \frac{\partial h}{\partial x} + \frac{\partial}{\partial x} \left[ -\frac{h^3}{3\mu} \frac{\partial p}{\partial x} + \frac{h^2}{2\mu} \tau_x \right] + \frac{\partial}{\partial y} \left[ -\frac{h^3}{3\mu} \frac{\partial p}{\partial y} + \frac{h^2}{2\mu} \tau_y \right] + \frac{\dot{m}}{\rho_l} = 0 \tag{2.4}$$

Equation (2.4) is the well-known Reynolds lubrication equation which describes the evolution of thin viscous, incompressible fluid films. In the chapter 3, we will discuss the functional dependence of $p \equiv p(h)$ and $\mu \equiv \mu(h, T)$ on temperature $T$ and film thickness $h$ for the lubricant. We will describe expressions for the net evaporation flux for both the disk ($\dot{m}_d$) and the slider ($\dot{m}_s$) lubricant films. We will also discuss the source of the traction boundary terms: $\tau_x(T)$ and $\tau_y(T)$, which are components of shear stress acting on the top surface of the lubricant film in the $x$ and $y$ directions respectively.

Equation (2.4) describes the evolution of the disk lubricant height $h_d(x, y, t)$ during HAMR writing ($h$ replaced by $h_d$, $U$ replaced by the disk linear velocity $u_d$, $\mu$ replaced by $\mu_d$, $p$ replaced by $p_d$, $\tau_x$ replaced by $\tau_{x,d}$, $\tau_y$ replaced by $\tau_{y,d}$, $T$ replaced by $T_d$, $\dot{m}$ replaced by $\dot{m}_d$). The governing equation for the slider lube thickness $h_s$ is also given by Eq. (2.4) ($h$ replaced by $h_s$, $U = 0$, $\mu$ replaced by $\mu_s$, $p$ replaced by $p_s$, $\tau_x$ replaced by $\tau_{x,s}$, $\tau_y$ replaced by $\tau_{y,s}$, $T$ replaced by $T_s$, $\dot{m}$ replaced by $\dot{m}_s$).

## 2.2 Governing Equation for Lubricant Vapor

The disk lubricant evaporates to generate vapor, which forms a dilute, binary mixture with air in the HDI. Consistent with the lubrication approximation, we assume that the

density of the lubricant vapor in the HDI, $\rho_v$ is independent of the normal co-ordinate $z$, i.e., $\rho_v \equiv \rho_v(x, y)$. We start with the continuity equation, integrated along the normal co-ordinate $z$, across the air bearing thickness $h_a$:

$$\frac{\partial}{\partial t}(\rho_v h_a) + \frac{\partial m_x}{\partial x} + \frac{\partial m_y}{\partial y} = \dot{m}_d + \dot{m}_s \tag{2.5}$$

Here $h_a \equiv (fh - h_s - h_d)$ is the height of the air bearing where $fh$ is the constant head-disk spacing at the NFT (Refer Figure 2.1). $m_x \equiv \int_{h_d}^{h_d+h_a} \rho_v v_{v,x} dz$ and $m_y \equiv \int_{h_d}^{h_d+h_a} \rho_v v_{v,y} dz$ are the lubricant vapor mass flow rates per unit length in the $x$ and $y$ directions respectively, obtained by integrating the product of lubricant density $\rho_v$ with the lubricant vapor velocity $v_{v,x}$ and $v_{v,y}$ in the $z$ direction across the air bearing clearance. $\dot{m}_d$ and $\dot{m}_s$ are the net evaporation mass fluxes from the disk and slider lubricant films respectively. Using Fick's Law for diffusion, the lubricant vapor velocity $v_{v,x}$ and $v_{v,y}$ can be expressed as

$$\rho_v v_{v,x} = \rho_v v_{m,x} - \rho_m D \frac{\partial m_v}{\partial x}$$
$$\rho_v v_{v,y} = \rho_v v_{m,y} - \rho_m D \frac{\partial m_v}{\partial y} \tag{2.6}$$

Here $v_{m,x}$ and $v_{m,y}$ are the air-lubricant vapor mixture velocities in the $x$ and $y$ directions, $\rho_m$ is the mixture density and $m_v \equiv \frac{\rho_v}{\rho_m}$. $D$ is the lubricant vapor diffusivity in air. We assume that the lubricant vapor in air is a dilute mixture so that the mixture velocity can be approximated by the air bearing velocity, $v_{m,x} \approx v_{a,x}$ and $v_{m,y} \approx v_{a,y}$ and that $\rho_m$ is approximately constant over the scale on which $\rho_v$ varies. With these assumptions, Fick's law can be re-written as

$$\rho_v v_{v,x} = \rho_v v_{a,x} - D \frac{\partial \rho_v}{\partial x}$$
$$\rho_v v_{v,y} = \rho_v v_{a,y} - D \frac{\partial \rho_v}{\partial x} \tag{2.7}$$

The lubrication assumption implies that $\rho_v$ and $\rho_m$ are independent of the normal co-ordinate $z$. Integrating across the air bearing thickness with this assumption, we get

$$m_x = \rho_v \int_{h_d}^{h_d+h_a} v_{a,x} dz - D h_a \frac{\partial \rho_v}{\partial x} = \rho_v q_x - D h_a \frac{\partial \rho_v}{\partial x}$$
$$m_y = \rho_v \int_{h_d}^{h_d+h_a} v_{a,y} dz - D h_a \frac{\partial \rho_v}{\partial y} = \rho_v q_y - D h_a \frac{\partial \rho_v}{\partial y} \tag{2.8}$$

Now we substitute these mass fluxes in the integrated continuity equation to get the governing equation for the lubricant vapor[8]

$$\frac{\partial}{\partial t}(\rho_v h_a) + \frac{\partial}{\partial x}(\rho_v q_x) + \frac{\partial}{\partial y}(\rho_v q_y) = \frac{\partial}{\partial x}\left(D h_a \frac{\partial \rho_v}{\partial x}\right) + \frac{\partial}{\partial y}\left(D h_a \frac{\partial \rho_v}{\partial y}\right) + \dot{m}_d + \dot{m}_s \tag{2.9}$$

6

Here $q_x \equiv \int_{h_d}^{h_d+h_a} v_{a,x} dz$ and $q_y \equiv \int_{h_d}^{h_d+h_a} v_{a,y} dz$ are the volume flow rates per unit length in the $x$ and $y$ directions, obtained by integrating the air bearing velocity $v_{a,x}$ and $v_{a,y}$ in the $z$ direction across the air bearing clearance.

Equation 2.9 is the governing equation for the lubricant vapor density in the air bearing. We assume that the effects of the lubricant vapor on the air bearing pressure, temperature and velocity can be neglected. Also, the lubricant as well as air bearing temperature is simply assumed to be equal to the average of the disk and slider temperatures $T_v \equiv (\frac{T_s+T_d}{2})$. Finally, the lubricant vapor density $\rho_v$ and partial pressure $p_v$ are assumed to be related by the ideal gas law

$$p_v = \frac{\rho_v R T_v}{M_w} \tag{2.10}$$

where $R$ is the molar universal gas constant and $M_w$ is the lubricant molecular weight. The first term in Eq. (2.9) models the unsteady lubricant vapor density change and dynamic air bearing height change. The next two terms on the LHS of Eq. (2.9) model the vapor convection effect due to the air bearing velocity. The effect of lubricant vapor diffusion in the air bearing layer is modeled by the first two terms on the RHS of Eq. (2.9). Finally, lubricant evaporation/condensation from the disk/slider is modeled by the last two terms of Eq. (2.9).

# Chapter 3

# Lubricant Transfer Model

## 3.1  Lubricant Property Models

In this chapter, we study the properties of nanoscale lubricant films used in HDDs such as surface tension, disjoining pressure, viscosity, diffusivity and vapor pressure. Perfluoropolyethers (PFPEs) are common lubricants used in the magnetic recording industry due to their favorable properties such as chemical stability, low volatility, thermal stability, and low viscosity. In this study, we consider the PFPE lubricant, Zdol 2000 (i.e. Molecular weight 2 kg/mol) for our simulations.

### 3.1.1  Thin Film Viscosity

The first question that needs to be answered in order to study the behavior of nanoscale lubricant films is if continuum theory can be used to describe the lubricant flow. This question was addressed by Karis et al. in[9]. Their experiments suggest that the flow of molecularly thin liquid films on a solid surface can still be described by the continuum theory with the adoption of an enhanced effective viscosity. In this section we discuss a theoretical model for this effective thin-film viscosity and comparison of this model with experimental data.

At high rotation rates of magnetic recording disks (5000-10000 RPM), a significant amount of lubricant coated on the disk spin-offs from the disk surface due to air shear stress on the free surface. Karis et al.[9] measured this spin-off and used this experimental data to determine the film thickness dependence of lubricant viscosity. Lubricant thickness was measured as a function of spin time at 10000 RPM on typical carbon overcoated magnetic recording disks initially lubricated with 1 to 13.5 nm of perfluoropolyether Zdol 4000.

The simplified form of the governing equation (2.4) in radial co-ordinates in a frame of reference which is rotating with the disk is given by[9]

$$\frac{\partial h}{\partial t} + \frac{1}{r}\frac{\partial}{\partial r}\left[r\frac{h^2}{2\mu}\tau_r\right] = 0 \tag{3.1}$$

Here $\tau_r$ is the radial component of the external shear stress acting on the lubricant (due to air). In this equation, the circumferential component of the air shear stress, $\tau_\theta$ and the centrifugal body force are assumed to negligible. Additionally, the lubricant is assumed to have a uniform pressure, and evaporation is ignored. An exact solution of the air flow problem is available for the case in which the column of air above the rotating disk is unbounded. The expression for the radial component of the air shear stress is given by[9]

$$\tau_r = \frac{r\omega\sqrt{\mu_a\rho_a\omega}}{2} \tag{3.2}$$

where $\mu_a$ and $\rho_a$ are the air viscosity and density, respectively, $r$ is the radius, and $\omega$ is the disk angular velocity. Hence, by combining equations (3.1) and (3.2), we get[9]

$$\frac{\partial h}{\partial t} = -\omega\sqrt{\mu_a\rho_a\omega}\frac{h^2}{2\mu} \tag{3.3}$$

Equation (3.3) was employed to calculate viscosity from the measured spin-off removal rate $\frac{\partial h}{\partial t}$ by Karis et al.[9] In reality, intermolecular van der Waal's forces between the substrate and the lubricant film cause the viscosity of the lubricant film to increase near the substrate as compared to its bulk value, i.e., the lubricant viscosity varies along the film thickness. However, Eq. (3.3) assumes that the viscosity is constant along the film thickness. Thus, the viscosity calculated from equation (3.3) is the viscosity that the fluid would have if it were actually constant throughout the film. Hence, the viscosity calculated from the spin-off removal rate with equation (3.3) is referred to as the effective thin-film viscosity $\mu = \mu(h,T)$.

The influence of this intermolecular interaction on the viscosity can be explained by Eyring's rate theory. Eyring reasoned that because some of the same intermolecular bonds are broken in a flow process as in a vaporization process, the activation energies of viscous flow can be estimated from vaporization energies. Karis[9] applied Eyring's rate theory to hard disk drive lubricants. The resulting thin film viscosity model is:

$$\mu(h,T) = \frac{N_A h_P}{V_l}exp\left(\frac{\Delta E_{vis}(h) - T\Delta S_{vis}(h)}{RT}\right) \tag{3.4}$$

where $N_A$ is Avogadro's number, $h_P$ is Planck's constant, $V_l$ is the molar volume of the lubricant, $R$ is the universal gas constant and $T$ is the lubricant temperature. $\Delta E_{vis}(h)$
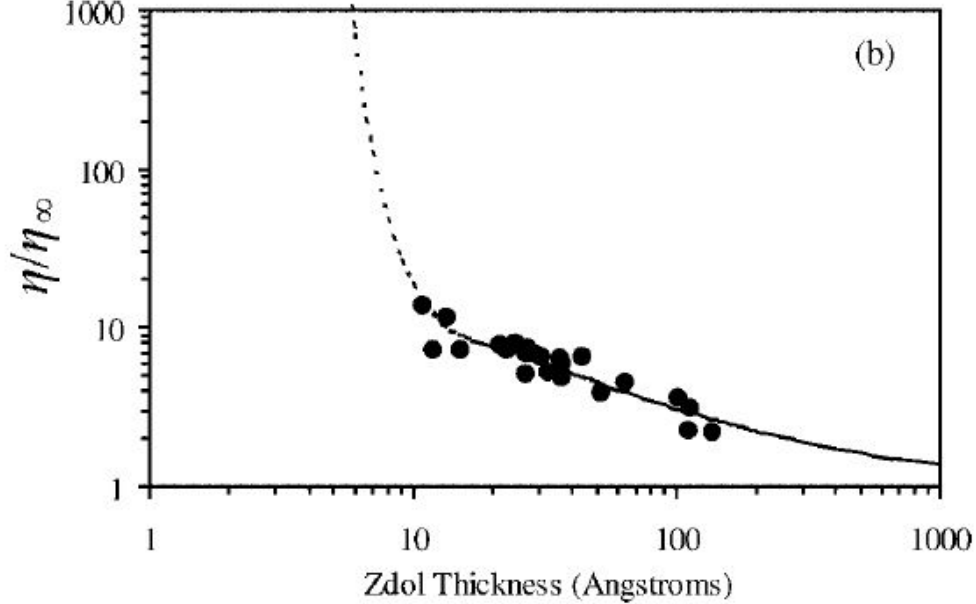
Figure 3.1: Lubricant viscosity as a function of film thickness for Zdol 4000. Reprinted by permission from Springer Nature (Tribology Letters)[9], Copyright (2001). Filled symbols are from the spin-off measurements using Eq. (3.3). The solid and dashed line are computed using Eq (3.4).

and $\Delta S_{vis}(h)$ are the flow-activation energy and entropy that depend on film thickness. The effective viscosity of Zdol 4000 as a function of film thickness based on this theoretical model (Eq. (3.4)) and comparison with the spin-off measurements (using Eq (3.3)) is shown in Fig. 3.1[9]. The viscosity of the disk lubricant $\mu_d \equiv \mu(h_d, T_d)$ is given by Eq. (3.4) with $h$ replaced by $h_d$ and $T$ replaced by $T_d$.

### 3.1.2  Disjoining Pressure

The concept of disjoining pressure was introduced by Derjaguin[10] and defined as the difference between the normal component of the pressure tensor in the liquid film and that of the bulk phase of the same liquid under the same thermodynamic conditions. Intermolecular forces (both van der Waals and others like electrostatic) have some finite range r. For a thick liquid film, molecules at the liquid-air interface experience intermolecular forces from liquid molecules in the film. However, for nanoscale films, as the film thickness becomes comparable to the range of intermolecular interaction r, the lubricant molecules at the lubricant-air interface experience intermolecular forces from both liquid molecules in the film and the molecules in the solid substrate. Hence, the hydrostatic pressure p in the thin liquid differs from the pressure of the bulk phase under the same thermodynamic conditions

10

(equal temperature and chemical potential). The difference between these two pressures is defined as the disjoining pressure. For a single-component liquid, the disjoining pressure may be determined as the derivative of the free energy per unit area of a thin layer, which arises from the effect of surface forces. Based on this definition, the disjoining pressure of disk lubricant $\Pi_d$ as a function of its thickness $h_d$ is given by[11][12]

$$\Pi_d(h_d) = -\frac{\partial \gamma_d^d}{\partial h_d} - \frac{\partial \gamma_d^p}{\partial h_d} = \Pi_d(h_d)^d + \Pi_d(h_d)^p = \frac{A_{VLS}}{6\pi(h_d + d_0)^3} + \Pi_d(h_d)^p \tag{3.5}$$

Here we consider two components of disjoining pressure and use the mischaracterizing nomenclature common in hard drive lubricant literature[13] - dispersive $\Pi_d^d$ and polar $\Pi_d^p$, based on the corresponding components of the thin film surface energy $\gamma_d^d$ and $\gamma_d^p$. The dispersive disjoining pressure $\Pi_d^d$ is a consequence of van der Waals interactions and has a $1/h^3$ dependence. Here $A_{VLS}$ is the Hamaker constant for the vapor-liquid-solid system and $d_0$ is a constant introduced to account for the molecular effect of the finite size of the atoms and molecules within the lubricant film. The oscillating polar component $\Pi_d^p$ is due to structural effects or non-van der Waals interactions introduced by the functional end-groups and is typically represented by a polynomial expansion. The coefficients of dispersive disjoining pressure ($A_{VLS} = 4.59 \times 10^{-20}$ J, $d_0 = 0.172$ nm) and polar disjoining pressure (curve-fitting parameters for polynomial expansion) of Zdol 2000 can be found in the paper by Sarabi and Bogy[14]. These coefficients are based on the methodology described by Karis & Tyndall[11] and the experimental data of surface energy of Zdol 2000 given by Tyndall et al.[12]

Some researchers[13] have questioned the assumptions made in the widely used contact angle method used to determine disjoining pressure in[11],[12]. While such methods seem to provide reasonable estimates of surface energies for solid surfaces, it has been cautioned that the values determined for disjoining pressure should not be taken as a true experimental measurement. In the absence of an accurate method for measuring disjoining pressure for actual lubricant/disk systems, we use the contact angle measurements in Tyndall et al.[12]

At nanometer scale head-disk clearances, the disk lubricant disjoining pressure is also influenced by the presence of the slider and the lubricant layer on the slider (of thickness $h_s$)[13,15,16]. The resulting expression for the disk lubricant disjoining pressure is given by:[17],[18]

$$\begin{aligned} \Pi_d(h_d, h_s) = -p_d &= \frac{A_{VLS}}{6\pi(h_d + d_0)^3} + \Pi_d(h_d)^p \\ &+ \frac{A_{VLS}}{6\pi(fh - h_d - d_0)^3} + \frac{A_{LVL}}{6\pi(fh - h_d - h_s - 2d_0)^3} \end{aligned} \tag{3.6}$$

Here $A_{LVL}$ is the Hamaker constant for the liquid-liquid interactions through vapor. In this study, we assume that $A_{LVL} \approx (2.1 \times 10^{-18})\gamma_\infty \approx 3 \times 10^{-20}$ J[16,19], where $\gamma_\infty = 15.8 \times 10^{-3}$

$J/m^2$ is the bulk surface energy of Zdol 2000. A detailed derivation of Eq. (3.6) was given by Forcada.[17]

### 3.1.3  Surface Tension

Whereas molecules deep within the liquid have neighbours on all sides, those within a distance of order r (where r is the range of intermolecular forces (see Section 3.1.2)) of the interface see neighbours on one side only. Thus, lubricant molecules at the interface experiences intermolecular attractions from one side only. The unbalanced intermolecular forces near an interface means there is a thermodynamic surface energy $\gamma_{LV}$ per unit area of liquid-vapor interface. This means that in order to bring more molecules to the surface and increase the area of the interface, an additional energy $\gamma_{LV}$ per unit of the added area needs to be applied to the system. For liquids, surface energy can be interpreted as a force per unit length that acts tangent to the interface, and this force is commonly called surface tension. The resultant stress due to surface tension can be decomposed into two components. The first component called Laplace pressure acts normal to the lubricant surface due to surface curvature and is given by

$$p_{lap}\boldsymbol{n} = (-\gamma \nabla \cdot \boldsymbol{n})\boldsymbol{n} \approx (\gamma \nabla^2 h)\boldsymbol{e_z} \tag{3.7}$$

Here we have used the quasi-parallel film assumption ($|\nabla h| \ll 1, \boldsymbol{n} \approx \boldsymbol{e_z}$). Previous studies by Dahl and Bogy[7] and Sarabi and Bogy[14] have shown that the effect of the Laplace pressure on lubricant evolution under HAMR is negligible, particularly for thin lubricant films ($\leq 1.2$ nm). Hence, in this study, the effect of Laplace pressure on the lubricant evolution is ignored in this study.

The second component called Maragoni stress[20] acts tangential to the lubricant surface due to spatial non-uniformity of surface tension. In this application, the variation in surface tension is due to the temperature gradient (also called "thermocapillary shear stress") and can be expressed as:

$$\boldsymbol{\tau} = \nabla\gamma - (\nabla\gamma \cdot \boldsymbol{n})\boldsymbol{n} \tag{3.8}$$

With the quasi-parallel film assumption ($|\nabla h| \ll 1, \boldsymbol{n} \approx \boldsymbol{e_z}$), the resultant shear stress on the disk lubricant can be expressed as:

$$\boldsymbol{\tau_d} = \tau_{x,d}\boldsymbol{e_x} + \tau_{y,d}\boldsymbol{e_y} = \frac{\partial\gamma}{\partial x}\boldsymbol{e_x} + \frac{\partial\gamma}{\partial y}\boldsymbol{e_y} = -c\left(\frac{\partial T_d}{\partial x}\boldsymbol{e_x} + \frac{\partial T_d}{\partial y}\boldsymbol{e_y}\right) \tag{3.9}$$

Here, $T_d \equiv T_d(x, y, t)$ is the disk temperature profile and $c \equiv -\frac{d\gamma}{dT}$ is assumed to be constant and equal to $0.06\ mN/(m^oC)$ for Zdol 2000[7].

### 3.1.4 Thin film Evaporation

Vapor pressure depends on the system temperature and the nature and strength of the intermolecular interactions that need to be overcome for a molecule to escape the condensed state and vaporize. The bulk liquid vapor pressure is typically expressed as a function of liquid temperature $T$ and molecular weight $M_w$ (i.e. $p_{vap,\infty}(T, M_w)$) and is estimated using the well-known Clausius-Clapeyron equation. $p_{vap,\infty}(T, M_w)$ for Zdol 2000 is given by Karis[24]. Independent of its origin, a pressure difference across an interface causes a change in the equilibrium vapor pressure from the bulk value at a given temperature (Kelvin Effect). In the case of thin lubricant films, the disjoining pressure contributes to a pressure difference across the lubricant-air interface, causing enhancement in the equilibrium vapor pressure. With the bulk vapor pressure known, the equilibrium thin film vapor pressure of the disk lubricant is determined using the following expression[7,21]:

$$\frac{p_{vap,film}}{p_{vap,\infty}} = exp\left(\frac{M_w}{\rho_l RT_d}\left[-\pi_d(h_d, h_s)\right]\right) \tag{3.10}$$

Here $\pi_d(h_d, h_s)$ is the disjoining pressure of the disk lubricant given by Eq. (3.6). Next, the net evaporation rate from the disk $\dot{m}_d$ is determined using the Hertz-Knudsen-Langmuir model[7,22] as:

$$\dot{m}_d = \alpha\sqrt{\frac{M_w}{2\pi RT_d}}(p_{vap,film}(h_d, h_s) - p_v) \tag{3.11}$$

where $\dot{m}$ is the net evaporation mass flux, $M_w$ is the lubricant molecular weight, $R$ is the molar universal gas constant, $T$ is the lubricant temperature and $\alpha$ is the accommodation constant. $p_{vap,film}$ is the equilibrium thin film vapor pressure and $p_v$ is the partial pressure of the lubricant vapor in air.

### 3.1.5 Convection and Diffusion

The lubricant convection model in Eq. (2.9) requires the air bearing velocity profiles in the $x$ and $y$ directions near the location of the NFT. Theoretically, this velocity profile can be obtained from an air bearing model for HAMR like CMLAir HAMR[23]. However, the air bearing model in[23] is rather coarsely meshed near the NFT location. Hence, due to the lack of accurate air velocity profiles very close to the NFT, we assume the following simple model for volume fluxes $q_x$ and $q_y$

$$q_x = u_d(fh - h_{0,d} - h_{0,s}) \quad q_y = 0 \tag{3.12}$$

Karis[24] used the Hirschfelder approximation to obtain the lubricant vapor phase diffusion coefficient:

$$D = 1.858 \times 10^{-4} \left( \frac{1}{M_w} + \frac{1}{M_a} \right)^{0.5} \frac{T_v^{1.5}}{P_a \sigma_i \Omega} \tag{3.13}$$

where $M_a$ and $M_w$ are the air and lubricant molecular weights and $P_a$ is the air bearing pressure. Expressions for collision diameter $\sigma_i$ and collision integral $\Omega$ can be found in[24].

## 3.2 Governing Equations for Lubricant Transfer

### 3.2.1 Governing Equation for the Disk Lubricant

The governing equation for the disk lubricant can be obtained by substituting Eqs. (3.4), (3.6), (3.9) and (3.11) in Eq. (2.4)

$$\frac{\partial h_d}{\partial t} + u_d \frac{\partial h_d}{\partial x} + \frac{\partial}{\partial x} \left[ \frac{h_d^3}{3\mu_d} \frac{\partial \pi_d}{\partial x} - \frac{h_d^2}{2\mu_d} c \frac{\partial T_d}{\partial x} \right] + \frac{\partial}{\partial y} \left[ \frac{h_d^3}{3\mu_d} \frac{\partial \pi_d}{\partial y} - \frac{h_d^2}{2\mu_d} c \frac{\partial T_d}{\partial y} \right] + \frac{\dot{m}_d}{\rho_l} = 0 \tag{3.14}$$

In this study, we have ignored the effect of the air bearing pressure and shear stress on the disk lubricant evolution. The timescale of disk lubricant evolution during HAMR writing is of the order of nanoseconds, while the effects of the air bearing pressure and shear stress are expected to be on the order of seconds[25]. In general, the net lubricant pressure is given by the sum of the disjoining pressure (Eq. (3.6)), the laplace pressure (Eq. (3.7)) and the air bearing pressure. However, with the latter two effects ignored, the net lubricant pressure is given by $p_d = -\Pi_d(h_d, h_s)$ (i.e. Eq. (3.6)). Similarly, the net lubricant shear stress $\boldsymbol{\tau_d}$ is, in general, given by the sum of the thermocapillary stress and the air shear stress. But, with air shear ignored, $\boldsymbol{\tau_d}$ is given by Eq. (3.9).

We use the same non-dimensionalization scheme as Dahl and Bogy[7].

$$h_d* = h_d h_{0,d} \quad x* = xL \quad y* = yL \quad \mu_d* = \mu_d \mu_0 \quad T_d* = T_d \Delta T_d + T_0 \tag{3.15}$$

Here $h_{0,d}$ is the initial disk lubricant thickness, $L$ is the disk temperature profile FWHM, $T_0$ is the ambient temperature, $\Delta T_d$ is the maximum prescribed disk temperature rise $T_{max,d} - T_0$ and $\mu_0 = \mu(T_0, h_{0,d})$. This choice of non-dimensional variables implies the following scales and coefficients:

$$t* = t t_s \quad \pi_d* = \pi_d p_s \quad t_s \equiv \frac{2\mu_0 L^2}{h_{0,d} c \Delta T_d}$$

$$p_s \equiv \frac{3}{2} \frac{c \Delta T_d}{h_{0,d}} \quad C_u \equiv \frac{2\mu_0 L u_d}{h_{0,d} c \Delta T_d} \quad S_d \equiv \frac{2\mu_0 L^2}{h_{0,d}^2 c \Delta T_d} \frac{\dot{m}_d}{\rho_l} \tag{3.16}$$

14

We now switch to a notation where quantities with an asterisk are dimensional and quantities without an asterisk are non-dimensional. The final non-dimensional governing equation for the disk lubricant is:

$$\frac{\partial h_d}{\partial t} + C_u \frac{\partial h_d}{\partial x} + \frac{\partial}{\partial x}\left[\frac{h_d^3}{\mu_d}\frac{\partial \pi_d}{\partial x} - \frac{h_d^2}{\mu_d}\frac{\partial T_d}{\partial x}\right] + \frac{\partial}{\partial y}\left[\frac{h_d^3}{\mu_d}\frac{\partial \pi_d}{\partial y} - \frac{h_d^2}{\mu_d}\frac{\partial T_d}{\partial y}\right] + S_d = 0 \qquad (3.17)$$

The initial condition is a uniform film of lubricant of prescribed thickness $h_{0,d}$. We use Neumann boundary conditions on the ends of our domain.

## 3.2.2 Governing Equation for the Slider Lubricant

Similarly, the final non-dimensional governing equation for the slider lubricant can be expressed as

$$\frac{\partial h_s}{\partial t} + \frac{\partial}{\partial x}\left[\frac{h_s^3}{\mu_s}\frac{\partial \pi_s}{\partial x} - \frac{h_s^2}{\mu_s}\frac{\partial T_s}{\partial x}\right] + \frac{\partial}{\partial y}\left[\frac{h_s^3}{\mu_s}\frac{\partial \pi_s}{\partial y} - \frac{h_s^2}{\mu_s}\frac{\partial T_s}{\partial y}\right] + S_s = 0 \qquad (3.18)$$

The initial condition is a uniform film of lubricant of thickness $h_{0,s}$. We use Neumann boundary conditions on the ends of our domain. It is worthwhile to highlight that $h_s$ is nondimensionalized with respect to $h_{0,d}$ and $T_s$ is non-dimensionalized with respect to $\Delta T_d$. Also, we assume that the FWHM of disk and slider temperature profiles are the same and equal to $L$.

## 3.2.3 Governing Equation for the Lubricant Vapor

The governing equation for the lubricant vapor density in the air bearing is given by Eq. 2.9. We use the following non-dimensionalization for the lubricant vapor equation (2.9):

$$\rho_v* = \rho_v \rho_l \quad h_a* = h_a h_{0,d} \quad q_x* = q_x q_0 \quad q_y* = q_y q_0$$
$$D* = D D_0 \quad q_0 \equiv \frac{L h_{0,d}}{t_s} \quad C_D \equiv \frac{t_s D_0}{L^2} \qquad (3.19)$$

Here $\rho_l$ is the density of the liquid lubricant and $D_0$ is the diffusivity at ambient temperature $T_0$ and pressure $p_0$ ($D_0 \equiv D(T_0, p_0)$). The spatial and temporal non-dimensionalization is the same as that for the disk/slider lubricant Eq. (3.15) and (3.16). We now switch to a notation where quantities with an asterisk are dimensional and quantities without an asterisk are non-dimensional. The final non-dimensional governing equation for the lubricant vapor is:

$$\frac{\partial}{\partial t}(\rho_v h_a) + \frac{\partial}{\partial x}(\rho_v q_x) + \frac{\partial}{\partial y}(\rho_v q_y) = \frac{\partial}{\partial x}\left(C_D D h_a \frac{\partial \rho_v}{\partial x}\right) + \frac{\partial}{\partial y}\left(C_D D h_a \frac{\partial \rho_v}{\partial y}\right) + S_d + S_s$$
$$(3.20)$$

## 3.3   Numerical Scheme

Equations (3.17), (3.18) and (3.20) are three coupled partial partial differential equations in the three unknows $h_s$, $h_d$ and $\rho_v$ (or equivalently $p_v$ through (2.10)). Equations (3.18) and (3.20) are discretized using a finite volume method (Hybrid Scheme)[26]. For the disk lubricant equation (3.17), we follow the method used by Dahl and Bogy[7] - the non-advective part of the equation is discretized using the Hybrid Scheme and the advective part is solved using the Cubic Interpolation Spline (CIP) scheme[27,28]. The resulting set of non-linear, coupled algebraic equations are solved iteratively to obtain the three solution profiles.

# Chapter 4

# Results

During the HAMR writing process, a complex laser delivery system integrated into the head is used to heat the media locally to its Curie temperature, causing the disk lubricant to deform, evaporate and subsequently condense at the NFT location on the slider. In this chapter, we present some preliminary simulation results to study the evolution of the lubricant film on the disk, the evaporated lubricant vapor in the air bearing and the condensed lubricant film on the slider under write conditions.

In our simulation, we assume an initially uniform film of Zdol 2000 ($M_w = 2$ kg/mol) of thickness $h_{0,d} = 1$ nm on the disk. The ambient conditions are assumed to be $T_0 = 25$ ºC and $p_0 = 101325$ Pa. The disjoining pressure experimental data is valid in the thickness range 0.2-2 nm, hence we assume the initial lubricant thickness on the slider ($h_{0,s}$) to be 0.2 nm. We prescribe a Gaussian temperature profile centered at the origin ($x = 0$ nm, $y = 0$ nm) with a peak of 500 ºC and FWHM of 20 nm on the disk. The slider temperature profile has the same FWHM but a peak of 310 ºC. The head-disk clearance $fh$ is set to 4 nm, so that the initial air bearing height ($h_{a,0}$) is 2.8 nm. We consider a linear disk speed $u_d$ of 12.5 m/s (correspoding to disk rotational velocity of 5400 RPM and radial distance of 22.215 mm) and a simulation time $t_f$ of 2 ns. The air bearing pressure at the NFT is set to 2.2 MPa. The peak disk/slider temperature, head-disk spacing and air bearing pressure data are approximately based on 15 mW TFC (Thermal Fly Height Control) Power and 2 mW NFT Power simulations using the CML HAMR code[23]. We consider the same slider Air Bearing Surface (ABS) design for the HAMR air bearing simulations as Dahl & Bogy[23].
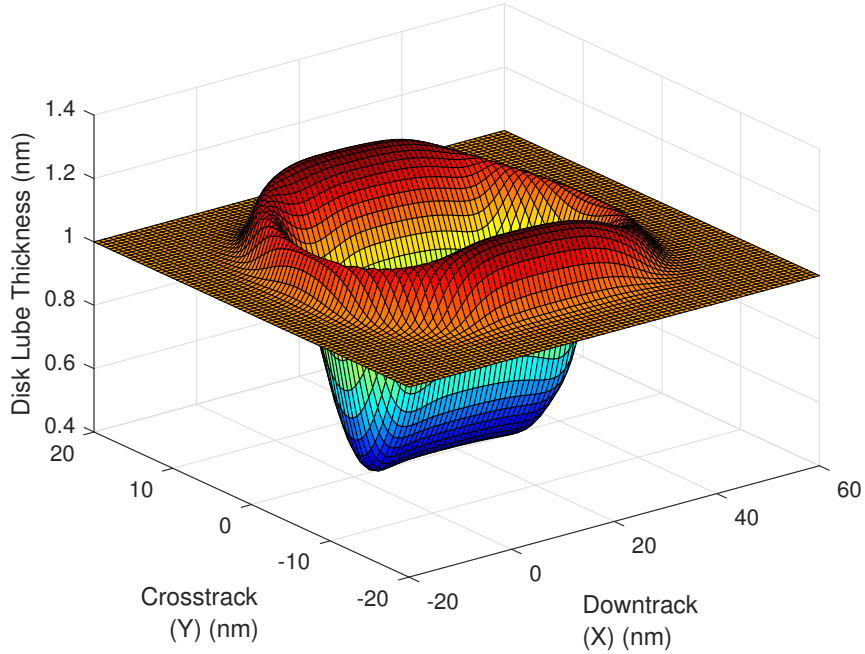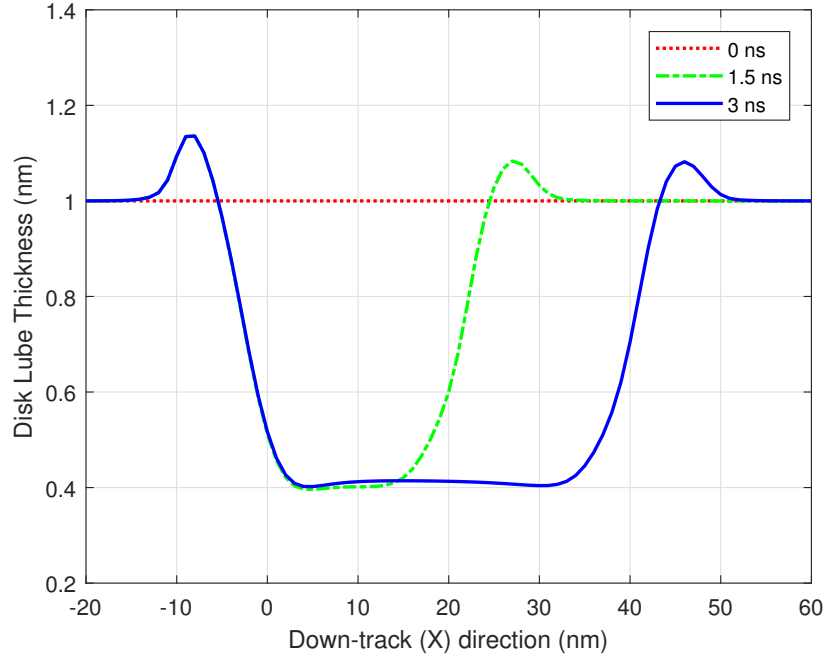
Figure 4.1: 3D plot of lubricant profile on disk after 3 ns of laser heating. $T_{max,d} = 500$ °C, $T_{max,s}$ = 310 °C, $U_d$ = 12.5 m/s, $h_{0,d}$ = 1 nm, fh = 4 nm, FWHM = 20 nm.

## 4.1 Disk Lubricant Thickness Profile

Figure 4.1 shows a 3D plot of the lubricant profile on the disk after 3 ns of laser heating. Projections of the disk lubricant profile along the down-track (x) and cross-track (y) directions are plotted in Figs. 4.2a & 4.2b. The stationary laser is centered at the origin ($x = 0$ nm, $y = 0$ nm), while the disk moves with a linear velocity of $U_d = 12.5$ m/s in the down-track direction. We see a central trough of depth 0.48 nm (at $y = 0$ nm) and side ridges of height 0.2 nm (at $y = \pm 10.5$ nm) in the cross-track disk lubricant profile in Fig. 4.2b, similar to those seen in previous works.[7] The disk lubricant trough depth does not change much over time, however, the length of the depleted region increases with time in Fig. 4.2a, due to the disk motion in the down-track direction.

The driving forces acting on the disk lubricant during HAMR writing are evaporation, thermocapillary stress and disjoining pressure. Evaporation leads to depletion of the disk lubricant. The disk temperature profile is a Gaussian curve centered at the origin ($x = 0$ nm, $y = 0$ nm) with a peak of 500 °C and FWHM of 20 nm. Since the disk temperature is maximum at the origin, the evaporation rate is also maximized here, and decreases as we move radially away from the origin. The thermocapillary stress is directly proportional to

(a) Down-track disk lubricant profile ($h_d$ vs $x$ at $y = 0$)
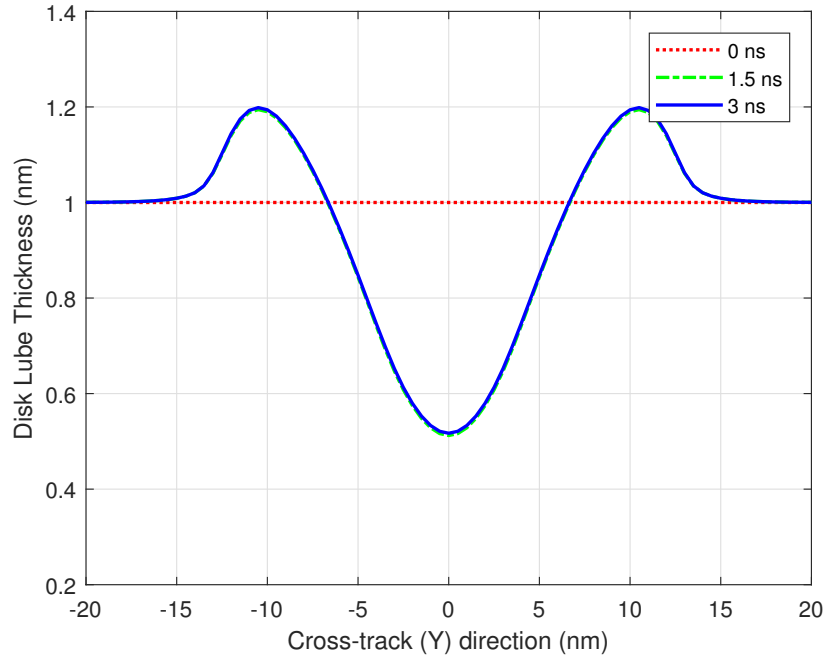


(b) Cross-track disk lubricant profile ($h_d$ vs $y$ at $x = 0$)

Figure 4.2: Down-track and cross-track lubricant profiles on disk at different times of laser heating. $T_{max,d} = 500$ °C, $T_{max,s} = 310$ °C, $U_d = 12.5$ m/s, $h_{0,d} = 1$ nm, fh = 4 nm, FWHM = 20 nm.

the spatial temperature gradient on the disk and hence tends to push the lubricant away from the origin. This causes the lubricant to deplete at the center (i.e. at the origin) and accumulate at the sides (at $y = \pm 10.5$ nm). In summary, the central trough in the cross-track profile is caused by evaporation as well as thermocapillary stresses, whereas the side ridges are largely due to thermocapillary stress.[7] Disjoining pressure acts as a restoring force, opposing the deformation of the lubricant.[7]

## 4.2  Slider Lubricant Thickness Profile

Figure 4.3 shows a 3D plot of the lubricant profile on the slider after 3 ns of laser heating. Projections of the slider lubricant profile along the down-track (x) and cross-track (y) directions are plotted in Figs. 4.4a & 4.4b. As disk lubricant depletion length increases with time (in down-track direction in Fig. 4.2a), lubricant accumulation on the slider also grows. Starting with a uniform film of 0.2 nm on the slider, the cross-track slider lubricant profile (Fig. 4.4b) shows a peak height of 0.84 nm at the end of 3 ns of heating.
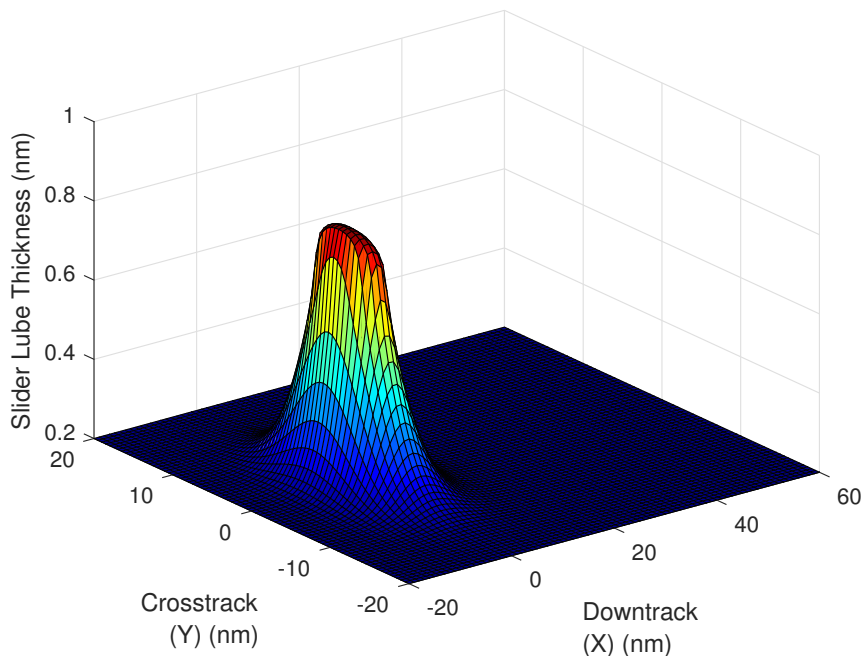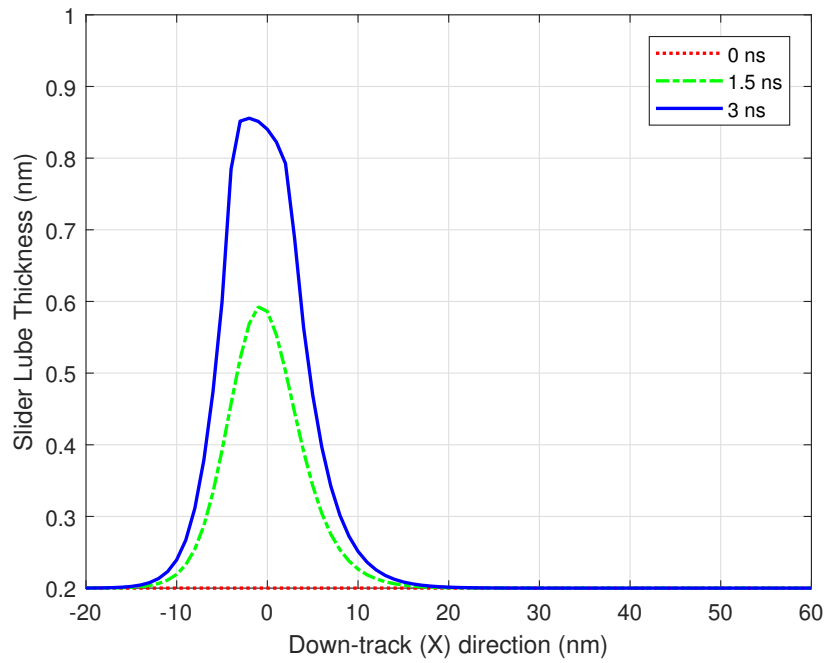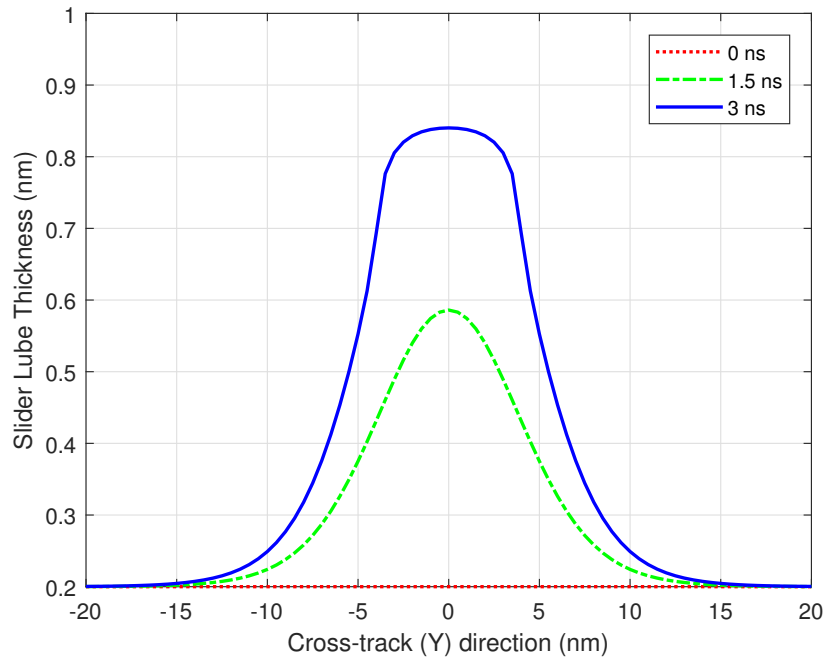


Figure 4.3: 3D plot of lubricant profile on slider after 3 ns of laser heating. $T_{max,d} = 500$ °C, $T_{max,s}$ = 310 °C, $U_d = 12.5$ m/s, $h_{0,d} = 1$ nm, fh = 4 nm, FWHM = 20 nm.

(a) Down-track slider lubricant profile ($h_s$ vs $x$ at $y = 0$)



(b) Cross-track slider lubricant profile ($h_s$ vs $y$ at $x = 0$)

Figure 4.4: Down-track and cross-track lubricant profiles on slider at different times of laser heating. $T_{max,d} = 500$ °C, $T_{max,s} = 310$ °C, $U_d = 12.5$ m/s, $h_{0,d} = 1$ nm, fh $= 4$ nm, FWHM $= 20$ nm.

## 4.3 Lubricant Vapor Pressure Profile

Figure 4.5 shows a 3D plot of the partial pressure of the lubricant vapor in the air bearing after 3 ns of laser heating. The lubricant vapor pressure is less than 0.1 MPa, while the air pressure at the NFT is 2.2 MPa, thereby justifying the dilute vapor assumption. At the origin ($x = 0$ nm, $y = 0$ nm), the disk and slider lubricant thicknesses at the end of 3 ns are 0.52 nm and 0.84 nm respectively. The thin film equilibrium vapor pressure (Eq. 3.10) at film thickness of 0.52 nm ($h_d$) and temperature of 500 °C ($T_d$) is 0.25 MPa and at 0.84 nm ($h_s$) and 310 °C ($T_s$) is 5 x $10^{-4}$ MPa. The partial pressure of the lubricant vapor phase at the origin ($p_v$) is 0.05 MPa. Thus, the large difference between the equilibrium vapor pressure of the disk lubricant and the head lubricant causes this relatively large mass flux from the disk to the head through the air bearing.
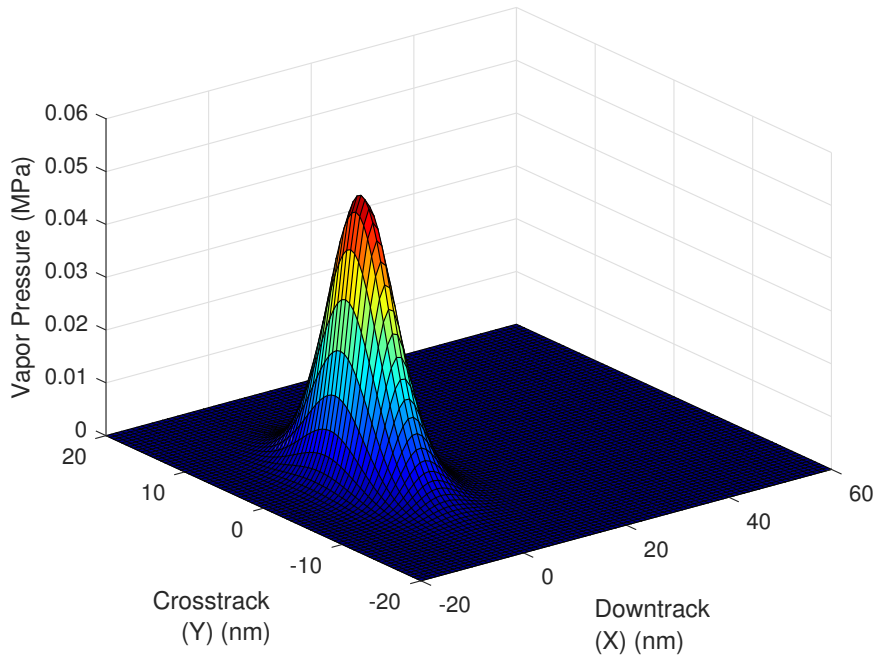


Figure 4.5: 3D plot of lubricant vapor phase partial pressure after 3 ns of laser heating. $T_{max,d} = 500$ °C, $T_{max,s} = 310$ °C, $U_d = 12.5$ m/s, $h_{0,d} = 1$ nm, fh = 4 nm, FWHM = 20 nm.

# Chapter 5

# Conclusion

## 5.1 Summary

We have developed a continuum mechanics based viscous model that predicts the lubricant transfer from the disk to the slider during HAMR writing. The model simultaneously determines the deformation and evaporation of the lubricant film on the disk, the convection and diffusion of the vapor phase lubricant in the air bearing and the evolution of the condensed lubricant film on the slider. Our model considers the effects of thermo-capillary stress (caused by the spatial temperature gradient) and thin-film viscosity of the disk and slider lubricant films. The model also accounts for molecular interactions between the disk-lubricant, slider-lubricant and lubricant-lubricant in terms of disjoining pressure. Disjoining pressure causes the equilibrium vapor pressure of the thin film to differ from its bulk value, which in turn, affects the evaporation rate. Our model also accounts for this thin-film evaporation/condensation rate. Our preliminary simulation results suggest that laser heating of the disk lubricant during HAMR writing causes several angstroms of lubricant depletion from the disk and subsequent condensation on the slider, in a timescale of nanoseconds for the PFPE lubricant, Zdol 2000.

## 5.2 Limitations and Future Work

We have presented preliminary simulation results for disk-to-head lubricant transfer during HAMR writing. Additional simulations need to be performed to study the effect of HAMR design parameters such as head temperature, media temperature, initial disk lubricant thickness, laser FWHM, lubricant molecular weight and head-disk spacing on the

disk-to-head lubricant transfer process. Our model can also be extended to other PFPE lubricants such as Ztetraol, so as to compare the performance of different lubricants during HAMR writing.

In this study, we have not considered the effects of thermal decomposition or lubricant polydisperity. Experiments suggest that the thermal decomposition of Zdol occurs at temperatures above 600 K[29]. Hence, in addition to evaporation, thermal decomposition could be another potential mechanism contributing towards lubricant depletion at high temperatures. PFPE lubricants are not chemically pure materials, but rather are a mixture of different molecular weight components. Since the rate of evaporation is a strong function of molecular weight, the degree of polydisperity will determine how the evaporation rate varies as lighter molecules will evaporate first[30].

The same physics of molecular interactions and their changes with temperature applies to surface tension and interfacial energetics. Marchon and Saito[31] considered the effect of a temperature dependent Hamaker constant on lubricant thermo-diffusion under laser heating. The model developed here can be improved by considering the effect of temperature on the Hamaker constants $A_{VLS}$, $A_{LVL}$ and $A_{SVL}$.

The lubricant is assumed to be a viscous, Newtonian fluid in this study. However, PFPE lubricants are viscoelastic fluids and can behave like viscous fluids or elastic solids or a combination of both depending on the flow timescale[24]. The model presented here can also be improved by considering viscoelastic effects on the lubricant transfer process. Finally, we do not consider the effect of lubricant slippage on the disk. At high shear strains, the no slip boundary conditions needs to be replaced by an appropriate slip boundary condition (such as Navier slip) to account for lubricant slippage.

# Bibliography

[1] Kryder, M., Gage, E., McDaniel, T., Challener, W., Rottmayer, R., Ju, G., Hsia, Y.T., Erden, M.: Heat assisted magnetic recording. IEEE transaction on magnetics. 96(11), 1810-1835 (2008)

[2] Marchon, B., Guo, X.C., Pathem, B.K., Rose, F., Dai, Q., Feliss, N., Schreck, E., Reiner, J., Mosendz, O., Takano, K., Do, H., Burns, J., Saito, Y.: Head-disk interface materials issues in heat-assisted magnetic recording. IEEE transaction on magnetics. 50(3), 3300607 (2014)

[3] Kiely, J.D., Jones, P.M., Y.Yang, Brand, J.L., Anaya-Dufresne, M., Fletcher, P.C., Zavaliche, F., Toivola, Y., Duda, J.C., Johnson, M.T.: Write-induced head contamination in heat-assisted magnetic recording. IEEE transactions on magnetics. 53(2), 3300307 (2016)

[4] Xiong, S., Wang, N., Smith, R., Li, D., Schreck, E., Dai, Q.: Material transfer inside head disk interface for heat assisted magnetic recording. Tribology Letters. 65-74 (2017)

[5] Sakhalkar, S.V. & Bogy, D.B.: A Model for Lubricant Transfer from Media to Head During Heat-Assisted Magnetic Recording (HAMR) Writing. Tribol. Lett. (2017).

[6] Oron, A., Davis, S., Bankoff, S.: Long-scale evolution of thin liquid films. Reviews of Modern Physics. 69, 931980 (1997)

[7] Dahl, J.B., Bogy, D.B.: Lubricant flow and evaporation model for heat-assisted magnetic recording including functional end-group effects and thin film viscosity. Tribology Letters. 52(1), 27-45 (2013)

[8] Wu, L.: A model for liquid transfer between two approaching gas bearing surfaces through coupled evaporation-condensation and migration dynamics. Journal of Applied Physics. 104, 014503 (2008)

[9] Karis, T., Marchon, B., Flores, V., Scarpulla, M.: Lubricant spin-off from magnetic recording disks. Tribology Letters. 11(3-4), 151-159 (2001)

[10] Derjaguin B.V., Churaev N., Muller V. Surface Forces. Consultants Bureau. Plenum Publishing Corporation, New York (1987)

[11] Karis, T., Tyndall, G.: Calculation of spreading profiles for molecularly-thin films from surface energy gradients. Journal of non-newtonian fluid mechanics 82(2), 287-302 (1999)

[12] Tyndall, G., Leezenberg, P., Waltman, R., Castenada, J.: Interfacial interactions of perfluoropolyether lubricants with magnetic recording media. Tribology Letters. 4(2), 103-108 (1998)

[13] Mate, C.M.: Taking a fresh look at disjoining pressure of lubricants at slider-disk interfaces. IEEE transaction on magnetics. 47(1), 124-130 (2011)

[14] Sarabi, M.S.G., Bogy, D.B.: Simulation of the performance of various PFPE lubricants under heat assisted magnetic recording conditions. Tribology Letters. 56(2), 293-304 (2014)

[15] Ambekar, R.P., Bogy, D.B., Dai, Q., Marchon, B.: Critical clearance and lubricant instability at the head-disk interface of a disk drive. Applied Physics Letters. 92(3), 033104 (2008)

[16] Pit, R., Marchon, B., Meeks, S., Velidandla, V.: Formation of lubricant moguls at the head/disk interface. Tribology Letters. 10(3), 133-142 (2001)

[17] Forcada, M.: Instability in a system of two interacting liquid films: Formation of liquid bridges between solid surfaces. The Journal of Chemical Physics. 98(1), 638 (1993)

[18] Christenson, H.: Capillary condensation due to vander waals attraction in wet slits. Physical Review Letters. 73(13), 1821-1824 (1994)

[19] Israelachvili, J.N.: Intermolecular and surface forces: revised third edition. Academic press (2011)

[20] Batchelor G.: An Introduction to Fluid Dynamics. Cambridge University Press, Cambridge, England (1967)

[21] Carey, V.P.: Liquid-Vapor Phase-Change Phenomena, 2 edn. Taylor and Francis Group, LLC, New York (2008)

[22] Rosenblatt, G.M.: Evaporation from Solids. In: N. Hannay (eds) Treatise on Solid State Chemistry, vol. 6A, chap. 3. Plenum Press, New York, pp. 165240 (1976)

[23] Dahl, J.B., Bogy, D.B.: Heat-assisted magnetic recording air bearing simulations that account for lateral air temperature variation. IEEE transactions on magnetics. 47(10), 2379-2382 (2011)

[24] Karis, T.: Lubricants for the disk drive industry. In: Rudnick L. (eds) Lubricant Additives: Chemistry and Applications, chap 22. CRC Press, Boca Raton, FL, pp. 523584 (2009)

[25] Wu, L.: Modelling and simulation of the lubricant depletion process induced by laser heating in heat-assisted magnetic recording system. Nanotechnology. 18(21), 215702 (2007)

[26] Patankar, S.: Numerical Heat Transfer and Fluid Flow. Hemisphere Publishing Corporation, New York (1980)

[27] Yabe, T., Aoki, T., Sakaguchi, G., Wang, P.: The compact CIP (cubic-interpolated pseudo particle) method as a general hyperbolic solver. Comput. Fluids (1991)

[28] Aoki T.: Multi-dimensional advection of CIP (cubicinterpolated propagation) scheme. Comput. Fluid Dyn. J. 4, 279291 (1995)

[29] Lei, R.Z., Gellman, A.J., Jones, P.: Thermal stability of fomblin z and fomblin zdol thin lms on amorphous hydrogenated carbon. Tribology Letters. 11(1), 15 (2001)

[30] Zhou, W., Zeng, Y., Liu, B., Yu, S., Hua, W., Huang, X.: Evaporation of polydisperse perfluoropolyether lubricants in heat-assisted magnetic recording. Appl. Phys. Express. 4(9), 095201 (2011)

[31] Marchon, B., Saito, Y.: Lubricant thermo-diffusion in heat assisted magnetic recording. IEEE transaction on magnetics. 48(11), 4471-4474 (2012)